Research Article | Vol. 26, No. 26 | 24 Dec 2018 | OPTICS EXPRESS 33613

Optics EXPRESS

Optical non-reciprocity induced by asymmetrical dispersion of Tamm plasmon polaritons in terahertz magnetoplasmonic crystals

QIAN YI SHI,[1] HUI YUAN DONG,[2] KIN HUNG FUNG,[3] ZHENG-GAO DONG,[1] AND JIN WANG[1,*]

[1]*School of Physics, Southeast University, Nanjing 211189, China*
[2]*School of Science, Nanjing University of Posts and Telecommunications, Nanjing 210003, China*
[3]*Department of Applied Physics, The Hong Kong Polytechnic University, Hong Kong, China*
[*]*jinwang@seu.edu.cn*

Abstract: Nonreciprocal light phenomena, including one-way wave propagation along an interface and one-way optical tunneling, are presented at terahertz frequencies in a system of magnetically controlled multi-layered structure. By varying the surface termination and the surrounding medium, it is found that the nonreciprocal bound or radiative Tamm plasmon polartions can be supported, manipulated, and well excited. Two different types of contributions to the non-reciprocity are analyzed, including the direct effect of magnetization-dependent surface terminating layer as well as violation of the periodicity in truncated multi-layered systems. Calculations on the asymmetrical dispersion relation of surface modes, field distribution, and transmission spectra through the structure are employed to confirm the theoretical results, which may potentially impact the design of tunable and compact optical isolators.

1. Introduction

Optical non-reciprocity refers to the asymmetrical characteristics in the transmission of the field when the source and detector are exchanged in their locations. This property is of immense importance for devices such as optical isolators [1–3], which allows light to propagate one single direction but blocks light in the opposite direction. The traditional way for realizing optical non-reciprocity relies on magneto-optical (MO) Faraday effects in a system based on ferrite materials, i.e. Yttrium Iron Garnet (YIG). However, owing to the intrinsic weakness of Faraday effects, such ferrite-based systems are generally bulky, thereby hindering the miniaturization of optical devices. Over the past two decades, enhanced nonreciprocal response is investigated in photonic crystals (PCs) by use of optical resonances. For example, resonant Faraday rotation response can be achieved by use of Bragg scattering in a magnetic photonic crystal waveguide [4], and also based on guided resonances [5], it is possible to obtain strong nonreciprocal response in a MO photonic crystal slab. Nonreciprocal behavior has also been demonstrated by considering numerous other techniques or methods, such as spatio-temporal dynamic modulation [6–9], opto-mechanical coupling effects [10–12] and the use of nonlinear optical processes [13–16].

It is well known that surface waves may possibly show nonreciprocal properties when the time-reversal symmetry is broken in a system [17–22]. Recently, Raghu and Haldane [17, 18] predicted firstly that the 2D MO PCs system can possess unidirectional photonic modes, which are direct analogs of chiral edge states of the electron in the quantum Hall effect. The field of such modes is bounded by the surface of PCs, exhibiting one-way wave propagation characteristics. Followed by the proposed theoretical prediction, several research groups [19, 20] realized and observed experimentally the electromagnetic one-way edge states in different MO PCs. The existence of one-way surface plasmon polaritons (SPPs) is also demonstrated in a plasmonic

#346834 https://doi.org/10.1364/OE.26.033613
Journal © 2018 Received 26 Sep 2018; revised 30 Nov 2018; accepted 30 Nov 2018; published 10 Dec 2018

Optics EXPRESS

waveguide under a static magnetic field [21]. However, the working frequency for this device is limited at visible spectral ranges, and meanwhile the required magnetic field is very high ($B > 10^3$ T) and not achievable to date.

On the other hand, Tamm plasmon-polaritons (TPPs) are surface localized waves bounded at the interface between a metal and a dielectric Bragg mirror and were proposed theoretically and confirmed experimentally by Kaliteevski and co-workers [23–25]. As for conventional SPPs, the confinement of TPPs on the metal side originates from the fact of the metal's negative dielectric constant at a frequency below its bulk plasma frequency. However, on the side of the Bragg mirror, the confinement is not due to total internal reflection but to the photonic band gap arising from the dielectric multilayer structure. Furthermore, TPPs can be supported in both the TE and TM polarizations and be excited without the use of special optical techniques such as prism or grating coupling. Due to the rapid growing interest in their properties, a number of potential applications on TPPs have been found in the realization of various optical components, such as absorbers [26], filters [27], optical switches [28, 29], polariton lasers [30–32], and single photon source [33] or the novel promising tool to engineer fluorophores emission [34–36].

Recently, great attention has been devoted to Terahertz (THz) science and technology due to its real-world applications, including sensing, imaging and wireless communications [37–39]. However, there still exists a challenge on the realization of high-performance, tunable, broadband and compact THz isolators, due to inadequate research of non-reciprocity mechanisms. In this work, we aim to examine significant non-reciprocity for TPPs at terahertz frequencies based on magnetically tunable multi-layered structure, when the external static magnetic field is less than 1 Tesla. It is shown that asymmetrical dispersions of TPPs can be obtained, leading to one-way wave propagation at the surface of semi-infinite structure or one-way optical tunneling when the structure becomes finite. Distinct nonreciprocal behavior can be tuned flexibly by varying geometrical or external parameters, i.e. surface terminations, the surrounding medium or external magnetic field. Moreover, the robustness of unidirectional propagation by the influence of a obstacle, as well as non-reciprocity in transmission related to loss effect of MO materials, is also investigated in our numerical simulations.

2. Model and methods

Let us start with a one-dimensional magnetoplasmonic crystal (MPC) as schematically illustrated in Fig. 1(a). The unit cell of the MPC consists of one magneto-optical active layer (ML), i.e. gyrotropic material, and one non-magnetic isotropic dielectric, with thicknesses d_1, d_2, and permittivities $\bar{\epsilon}_1$, ϵ_2, respectively. The external static magnetic field is applied along $-z$ direction, forming a Voigt configuration with magnetization in the plane of the MPC interface and perpendicular to the wave vector of TPPs. The optical property of ML is characterized by a permittivity tensor,

$$\bar{\epsilon}_1 = \begin{pmatrix} \epsilon_1 & i\Delta_1 & 0 \\ -i\Delta_1 & \epsilon_1 & 0 \\ 0 & 0 & \epsilon_1' \end{pmatrix}. \tag{1}$$

We take the following parameters for ML, i.e. $\epsilon_1 = \epsilon_\infty[1 - \omega_p^2(1 + i\alpha/\omega)/((\omega + i\alpha)^2 - \omega_c^2)]$, $\Delta_1 = -\epsilon_\infty\omega_p^2\omega_c/[\omega((\omega + i\alpha)^2 - \omega_c^2)]$ and $\epsilon_1' = \epsilon_\infty[1 - \omega_p^2/(\omega(\omega + i\alpha))]$. Here ϵ_∞ is the high-frequency permittivity, ω_p is the plasma frequency of ML, the collision frequency α characterizes loss strength in the ML, $\omega_c = eB/m^*$ is the cyclotron frequency, e is the electron charge, and m^* is the effective mass of electrons. Here we take a typical kind of semiconductor material for the ML layer, i.e. the indium antimonide (InSb), which can have a permittivity at THz frequencies similar to that of metals at optical frequencies, therefore using the Drude model [40, 41] for the permittivity of ML layer. It should be noted that the studied nonreciprocal behavior throughout

Optics EXPRESS

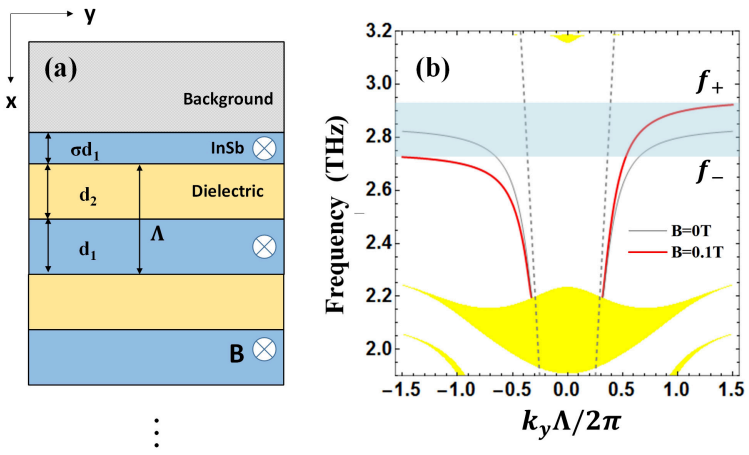

Fig. 1. (a) Schematic diagram of the proposed MPC structure, formed by alternating magneto-optical active [permittivity $\bar{\epsilon}_1$] and isotropic dielectric layers [permittivity ϵ_2]. The semi-infinite MPC structure with a top magneto-active layer is embedded into a kind of homogeneous background dielectric material with its permittivity ϵ_b. (b) Dispersion of bound TPPs at the surface of MPCs. Gray and red lines correspond to the TPPs solutions when the external magnetic field is absent [B = 0T] or present [B = 0.1T], respectively. f_+ and f_- denote respectively the cutoff frequencies where the forward- and backward-propagating modes vanish, then representing the one-way wave propagation by light blue region. Yellow and white regions correspond to pass-bands and stop-gaps of an infinite MPC. Light lines for the background material are also shown by dotted lines.

the paper is only limited to the case of TM-polarized light beam (magnetic field along z direction), because the TE mode solutions (electric field along z direction) for this system still possess time-reversal symmetry and Lorentz reciprocity. And the $e^{-i\omega t}$ time-dependent convention for harmonic field is used in this work.

The entire MPC structure is embedded into a kind of homogeneous surrounding material with permittivity ϵ_b. To study wave propagation behavior in this system, we may firstly find the solution of the band structure for 1D infinite periodic structure of MPCs by using standard transfer-matrix approach [42,43]. Let us consider a unit cell by starting from the interface of ML, and finishing the next such location after going through a full period $\Lambda = d_1 + d_2$, and the total transfer matrix $\hat{T}$ associated with such a particular choice of the unit cell gives $\hat{T} = \hat{P}_1\hat{M}_{21}\hat{P}_2\hat{M}_{12}$. $\hat{M}_{ij}$ is the interface matrix associated with the magnetic field at the interface between the layer i and j, taking the following form

$$\hat{M}_{ij} = \frac{\epsilon_j^2 - \Delta_j^2}{2\epsilon_j k_{xj}} \begin{pmatrix} F_j^* + F_i & F_j^* - F_i^* \\ F_j - F_i & F_j + F_i^* \end{pmatrix}, \tag{2}$$

where $F_m = (\epsilon_m k_{xm} + i\Delta_m k_y)/(\epsilon_m^2 - \Delta_m^2)$, $m = i, j$. The propagation matrix $\hat{P}_m = \mathrm{diag}[e^{ik_{xm}d_m}, e^{-ik_{xm}d_m}]$ describes the phase shift of the propagation wave in the m-th layer. By solving the eigenvalue problem on the matrix $\hat{T}$,

$$\hat{T}\begin{pmatrix} a_0 \\ b_0 \end{pmatrix} = e^{iK\Lambda}\begin{pmatrix} a_0 \\ b_0 \end{pmatrix}. \tag{3}$$

one can obtain the Bloch modes for the infinite MPC, where K is the Bloch wave vector.

Since the photonic band structure is only associated with the eigenvalues of transfer matrix, which is independent of the particular choice of a unit cell, one can consider a more general transfer matrix T_σ with a top layer, i.e. MO material with thickness σd_1 ($\sigma \in [0, 1]$, a geometrical parameter determining the truncation of the terminating layer of MPCs), which is given by $\hat{T}_\sigma = \hat{P}_\sigma^{-1}\hat{T}\hat{P}_\sigma$, where $\hat{P}_\sigma = \mathrm{diag}[e^{ik_{x1}\sigma d_1}, e^{-ik_{x1}\sigma d_1}]$. That is, $\hat{T}_\sigma$ and $\hat{T}$ have the same eigenvalues, and the eigenvectors for them satisfy the relations

$$\begin{pmatrix} a_\sigma \\ b_\sigma \end{pmatrix} = \hat{P}_\sigma^{-1} \begin{pmatrix} a_0 \\ b_0 \end{pmatrix}. \tag{4}$$

With the boundary condition that the tangential field components should be continuous across the interface, one can find the dispersion relation for TPPs,

$$q_b = ik_{x1}\frac{\epsilon_b\epsilon_1}{\epsilon_1^2 - \Delta_1^2}\frac{T_{12}e^{-2ik_{x1}\sigma d_1} + T_{11} - e^{iK\Lambda}}{T_{12}e^{-2ik_{x1}\sigma d_1} - T_{11} + e^{iK\Lambda}} - k_y\epsilon_b\frac{\Delta_1}{\epsilon_1^2 - \Delta_1^2}, \tag{5}$$

where q_b is defined as

$$q_b = \sqrt{k_y^2 - (\frac{\omega}{c})^2\epsilon_b}, \tag{6}$$

describing the wave decay rate in the background material.

Eigenmode solutions of Eq. (5) for our proposed structure could be found by using a commercial root solver (*Mathematica* FindRoot), to search the numerical root k_y of Eq. (5) at a fixed frequency. The non-reciprocity of TPPs which comes from the contribution of the first and second item on the right hand of Eq. (5) will be analyzed below.

3. One-way wave propagation at the interface of semi-infinite MPCs

Without loss of generality, we consider a typical kind of semiconductor material for the ML layer, i.e. the indium antimonide (InSb), the dielectric layer in the MPC, i.e. germanium (Ge) with high permittivity $\epsilon_2 = 16$ in THz region, which can provide good index contrast with InSb, thereby forming the band gap of the MPC, and low-loss background materials SiO_2 with permittivity $\epsilon_b = 4$ in the THz region for our calculation. The corresponding parameters of InSb at room temperature are taken as $m^* = 0.014m_0$ (m_0 is the free electron mass in vacuum), $\omega_p = 2 \times 10^{13}$ rad/s, and $\epsilon_\infty = 15.68$ [40,44]. We neglect the influence of the absorption in InSb by setting $\alpha = 0$ for initial calculations. The MO and dielectric layer have identical thickness with $d_1 = d_2 = 10\mu m$ throughout this work.

Fig. 1(b) depicts regions of photonic pass-bands (yellow regions) and stop-gaps (white regions), together with the dispersion of the forward ($k_y > 0$) and backward ($k_y < 0$) TPPs, where the surface termination is the InSb layer with $\sigma = 1$. In the absence of external magnetic field, $B = 0$ T, modes solution of TPPs is symmetrical and reciprocal, $f(k_y) = f(-k_y)$. However, when the magnetic field turns on, i.e. $B = 0.1$ T, it is seen that there exists distinct and asymmetrical TPPs modes with $f(k_y) \neq f(-k_y)$, and the branches of forward and backward TPPs approach and vanish, respectively, at different cutoff frequencies f_+ and f_-, which implies the THz waves in the frequency region of $[f_-, f_+]$ (the light blue region) can only propagate forward. For the range of results shown, the dispersion curves of TPPs lie in the band gap of the MPC and simultaneously outside the light cone of the surrounding medium. This indicates the associated modes are localized at the surface of MPC, and meanwhile not accessible to direct excitation by incident radiation.

As a direct illustration of wave transport properties for our system, we plot in Fig. 2 the out-of-plane magnetic field profile by using a finite element solver (COMSOL Multiphysics).

Optics EXPRESS

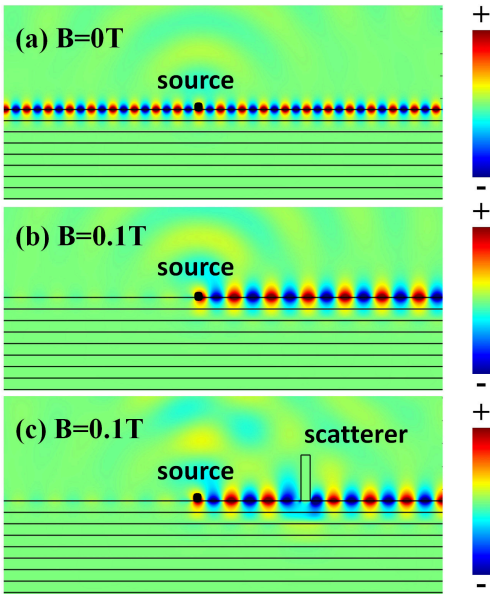

Fig. 2. Steady-state field distribution H_z at a frequency $f = 2.8$ THz with the applied magnetic field (a) $B = 0$T; (b) $B = 0.1$T, in the absence of the scatterer; (c) $B = 0.1$T, when a large PEC obstacle [height $40\mu m$ and width $8\mu m$] is inserted. The line source at the interface is marked with "•" in the figure.

A magnetic line current as the source is located at the surface of the MPC, radiating waves of various wave vectors. Those matching up with the dispersion curves may be picked up to excite the TPPs. The working frequency is set to $f = 2.8$ THz. As expected, surface waves, propagating forward or backward, are both well excited shown in Fig. 2(a), when the external static magnetic field is absent. In contrast, with the introduction of magnetic field, i.e. $B = 0.1$ T, the source radiates forward, and only along a single direction [Fig. 2(b)], implying the excitation of one-way TPPs identical with the prediction shown in Fig. 1(b). Moreover, the unusual property of such one-way edge mode on strong suppression of backscattering is also examined in Fig. 2(c). A slab of perfect electrical conductor (PEC) is inserted on the interface, and it is observed that forward propagating waves choose another route to go around the obstacle to avoid being backscattered.

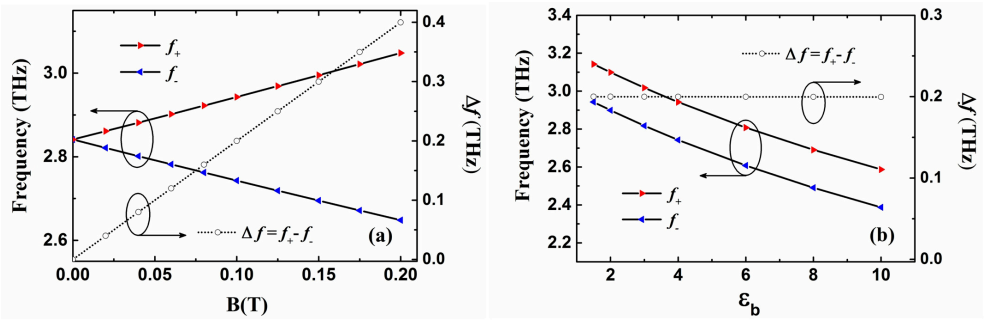

Fig. 3. Effect of (a) applied magnetic field B and (b) the permittivity ϵ_b of the background material on the cutoff frequency f_+ and f_-, and the bandwidth $\Delta f = f_+ - f_-$ of one-way wave propagation band. Note that $\epsilon_b = 4$ and $B = 0.1$T are used in (a) and (b), respectively. Other parameters are the same as Fig. 1.

Optics EXPRESS

The performance of the one-way propagating frequency band may be affected by geometrical parameters or external factors applied to the proposed system. Next, We calculate the cutoff frequencies of the forward (f_+) and backward (f_-) propagating modes, as well as the one-way transport regions, as a function of the applied magnetic field and permittivity of surrounding medium, shown in Fig. 3(a) and 3(b), respectively. With the increase of magnetic field, from 0 T to 0.2 T, the cutoff frequency starts to experience a splitting, giving rise to an increase of f_+ but a decrease in f_-. Consequently, the bandwidth $\Delta f \equiv f_+ - f_-$ of one-way propagating band exhibits a nearly linear variation from 0 to 0.4 THz, as the magnetic field increases. On the other hand, it depends little on the permittivity ϵ_b of the surrounding medium as seen in Fig. 3(b). Both f_+ and f_- decrease dramatically as ϵ_b increases from 1.5 to 10, but $\Delta f = 0.2$ THz remains almost unchanged.

We remark that in this regime, the field [seen from Fig.2] is strongly localized at the interface and just penetrates into the first layer of multilayer systems. Therefore, such non-reciprocity on TPPs develops mainly from contribution of the magnetization effect in the top layer of MPCs, directly related to the second item in Eq. (5). Meanwhile, in the limit of $k_y \gg \omega/c$, the TPPs tends to be far away from the photonic band edge, and our proposed system in Fig. 1(a) may be considered as a simple waveguide structure formed at the interface of MO and background materials. Under this circumstance, the dispersion for the interface mode is given by

$$q_b = -\frac{\epsilon_b}{\epsilon_1^2 - \Delta_1^2}(k_y\Delta_1 + k_{x1}\epsilon_1) \tag{7}$$

and the cutoff frequencies of the forward and backward propagating mode f_+ and f_- can be expressed analytically as [21, 41]

$$f_+ = \frac{1}{2\pi}\left[\sqrt{\frac{\omega_c^2}{4} + \frac{\epsilon_\infty\omega_p^2}{\epsilon_b + \epsilon_\infty}} + \frac{\omega_c}{2}\right], \tag{8}$$

$$f_- = \frac{1}{2\pi}\left[\sqrt{\frac{\omega_c^2}{4} + \frac{\epsilon_\infty\omega_p^2}{\epsilon_b + \epsilon_\infty}} - \frac{\omega_c}{2}\right]. \tag{9}$$

Thereby, the one-way-propagating bandwidth $\Delta f = \omega_c/2\pi$ is proportional to the magnetic field B, and independent of the permittivity of the surrounding medium, which is in excellent agreement with the results shown in Fig. 3.

We turn to investigate in Fig. 4 the impact of the surface termination by vary σ on the manipulation of TPPs. As the thickness of the top layer decreases from $\sigma = 0.8$ to 0.1, the cutoff frequencies f_+ and f_- move to higher ones, and the bandwidth Δf tends to zero, resulting in weaker non-reciprocity effect shown in Fig. 4. Nevertheless, at smaller σ, i.e. $\sigma < 0.5$, it is seen that there exists the radiative mode solutions for nonreciprocal TPPs inside the light cone of surrounding medium. We explain the formation of such radiative modes as below: when the top layer InSb layer shrinks to be a thin film, i.e. $\sigma < 0.5$, the localized field for interface modes starts to extend into the multilayer structure more deeply than in the case of $\sigma = 1$ shown in Fig. 3, the above mode of simple waveguide structure becomes not applicable, and new solutions including radiative modes may arise within the band gap of the MPCs. It should be noted that, different from the completely localized modes, the field for those radiative TPPs is not well confined at the interface, and can propagate in the background material.

4. One-way optical tunneling through finite-size MPCs

We proceed to explore the possibility to see a kind of completely localized TPPs with non-reciprocity, which are different from those shown in Fig. 1(b). They may be excited directly by

Optics EXPRESS

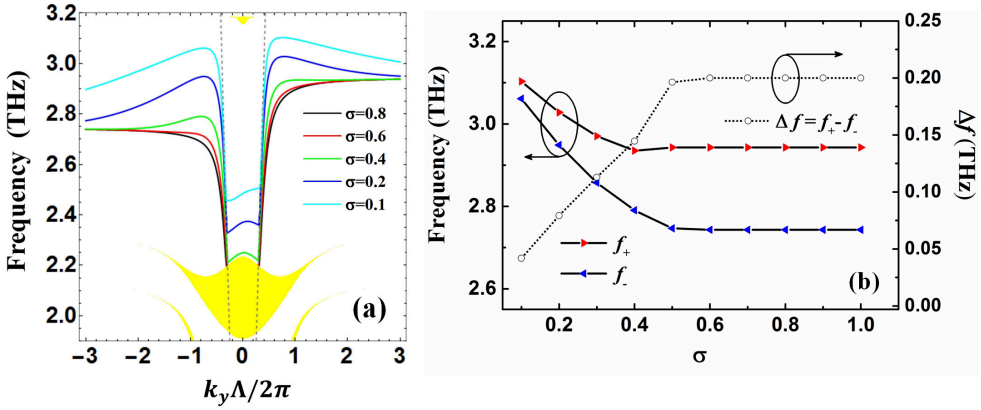

Fig. 4. (a) Dispersion for bound (or radiative) TPPs lying outside (inside) the light cone for the background material by tuning the surface terminating layer from $\sigma = 0.8$ to $\sigma = 0.1$. (b) Effect of surface terminating layer on the cutoff frequency f_+ and f_-, and the bandwidth $\Delta f = f_+ - f_-$ of one-way wave propagation band. Note that $\epsilon_b = 4$ and $B = 0.1$T are used in (b). Other parameters are the same as Fig. 1.

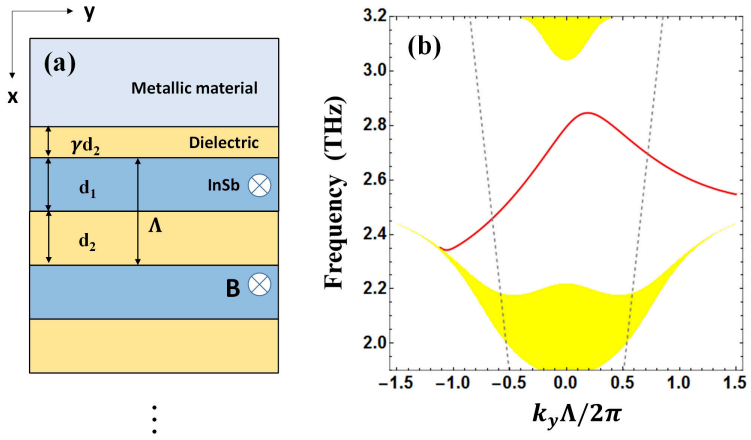

Fig. 5. (a) The schematic diagram is the same as Fig. 1(a) except that the top layer of the MPC and the surrounding materials are replaced by the dielectric and metallic material, respectively. (b) Dispersion for TPPs [the red line] consists of radiative solutions lying inside the light cone for the background material (with permittivity, $\epsilon_e = 16$). The applied magnetic field $B = 0.3$ T and the parameter γ for surface terminating layer is set to $\gamma = 0.4$. All other parameters and settings are the same as in Fig. 1.

incident plane waves. Based on the previous system in Fig. 1(a), we simply change the surface termination layer from magnetized InSb to the dielectric, and simultaneously the background from dielectric to the semiconductor material, i.e. unmagnetized InSb, as shown in Fig. 5(a). The parameter γ is used to tune the thickness of top dielectric layer of the MPC. All other geometrical parameters and settings remain unchanged. Correspondingly, by replacing the ϵ_1, σ by ϵ_2, γ, respectively, and meanwhile setting Δ_1 to be zero in Eq. (5), we can obtain the dispersion for

Optics EXPRESS

TPPs in this system shown in Fig. 5(a),

$$q_b = ik_{x2}\frac{\epsilon_b}{\epsilon_2}\frac{T_{12}e^{-2ik_{x2}\gamma d_2} + T_{11} - e^{iK\Lambda}}{T_{12}e^{-2ik_{x2}\gamma d_2} - T_{11} + e^{iK\Lambda}}, \tag{10}$$

where the transfer matrix $\hat{T}$ is also changed by $\hat{T} = \hat{P}_2\hat{M}_{12}\hat{P}_1\hat{M}_{21}$.

Likewise with Fig. 1(b), we plot in Fig. 5(b) the complete dispersion of forward and backward TPPs with a particular case of the external magnetic field $B = 0.3$ T and the parameter $\gamma = 0.4$. Asymmetrical and nonreciprocal TPPs [$f(k_y) \neq f(-k_y)$] are supported. Here, another type of contribution to the non-reciprocity of TPPs is revealed. It comes from the periodic violation of MPCs due to the surface termination [42,43], which results in the removal of the spatial symmetry for the MPCs structure, i.e. the mirror reflection symmetry. The non-reciprocity for TPPs may be directly seen from Eq. (10), in which the off-diagonal elements for the transfer matrix show asymmetrical properties, i.e. $T_{12}(k_y) \neq T_{12}(-k_y)$. It is emphasized that the Bloch band for 1D infinite two-component MPCs remains symmetrical, i.e. the Bloch number $K(k_y) = K(-k_y)$, due to the maintenance of spatial symmetry induced by periodicity of the structure. Notice that such TPPs mode solutions are bounded at the interface. The wave evanescent decay in the semiconductor is due to the negative dielectric constant, and meanwhile waves are falling within the band gap of MPCs. The lightlines for the dielectric material (permittivity ϵ_2) are also shown by dotted lines. The localized TPPs lying inside the light cone are expected to be directly excited by incident plane waves propagating at the dielectric.

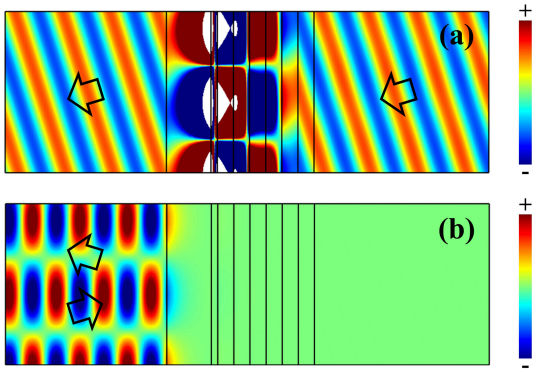

Fig. 6. Steady-state field patterns H_z for the finite-size structure consisting of a unmagnetized InSb layer (with thickness $a = 28\mu m$) on the surface of a 3-period MPC plus with a dielectric first layer under the back illumination (a) and front illumination (b), when the incident angle θ is chosen to be $\theta = 17.72^0$. The proposed finite-size structure is embedded into a uniform surrounding medium with permittivity $\epsilon_e = \epsilon_2 = 16$. Here $f = 2.67$ THz is used. Other parameters are identical with those in Fig. 5. In (a), the TPPs are well excited at the interface between non-magnetized InSb and MPCs, exhibiting strong enhancement on the magnetic field by the white color with its magnitude beyond the scope of the colorbar.

The excitation of such nonreciprocal TPPs is further confirmed by using COMSOL Multiphysics. We show in Fig. 6 the steady-state field patterns for a finite structure consisting of a unmagnetized InSb layer (with thickness $a = 28\mu m$) on the surface of three complete period MPCs plus with a first dielectric layer ($\gamma = 0.4$), in the presence of external incident radiation. Counterpropagating plane waves are incident from the surrounding dielectric material, with its permittivity, i.e. $\epsilon_e = \epsilon_2 = 16$. Other parameters are chosen with $B = 0.3$T and $f = 2.67$ THz. For the case of backward incidence, at a particular incident angle $\theta = -17.72^0$, strong field enhancement is seen at the surface of MPCs, and backward TPPs ($k_y < 0$) is well excited, giving rise to

Optics EXPRESS

full transmission through the whole structure [Fig. 6(a)]. In contrast, for the case of forward incidence, $\theta = +17.72^0$ [Fig. 6(b)], strong reflection is observed, resulted from the suppression of the excitation of forward TPPs ($k_y > 0$). Therefore, one-way optical tunneling through such a finite-size structure could be achieved. Notice that other selection for the thickness of unmagnetized InSb has no intrinsic influence on the non-reciprocity effect, but change slightly the intensity of light tunneling.

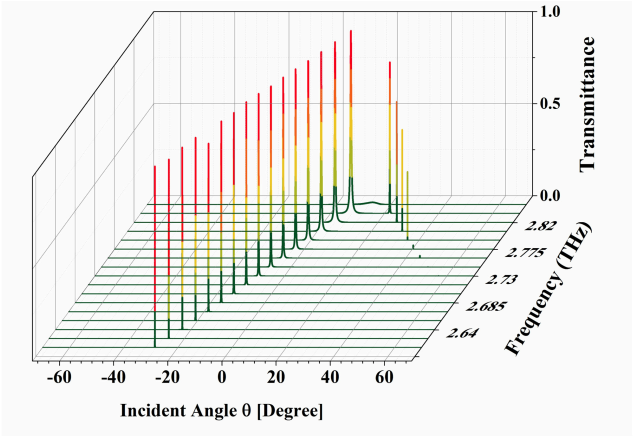

Fig. 7. Nonreciprocal transmittance T through the finite-size structure in Fig. 6.

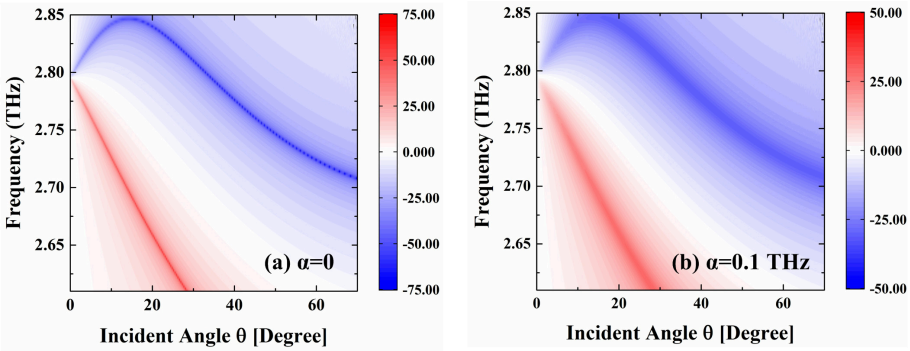

Fig. 8. The calculated isolation spectra for positive and negative incident angles when the loss in ML is absent (a) $\alpha = 0$, and present (b) $\alpha = 0.1$ THz.

As a validation of the above results, we can also directly determine the response of a finite structure illuminated by light by using transfer-matrix formalism. Figure 7 presents the transmittance through the same structure as Fig. 6 as a function of incident angle θ and frequency ω. It is observed that there exists distinct and asymmetrical transmission peaks, $T(\theta) \neq T(-\theta)$, over a certain of frequency range around $2.46 - 2.85$ THz. Such pronounced non-reciprocity of transmittance reveals that the optical properties are dependent of the specific direction, which is not observed in nonmagnetic, linear, and time-independent structures. Moreover, the transmission peaks could map well onto the dispersion curves for TPPs shown in Fig. 5 (b). Thus, the nonreciprocal character of TPPs may bring the directional dependence in transmission and result in one-way behavior for this finte-size system.

For the purpose of clearly demonstrating the performance of the non-reciprocity in transmission, which is strongly dependent on the incident angle of light, we define the isola-

Optics EXPRESS

tion between the forward transmittance $T(\theta)$ and backward transmittance $T(-\theta)$ expressed by $Iso = 10log[T(-\theta)/T(\theta)]$ and show in Fig. 8 the isolation spectra as a function of frequency and the incident angle θ of light illumination. Here we take a particular case with the applied magnetic field $B = 0.3$ T. In the absence of loss in ML, $\alpha = 0$ [Fig. 8(a)], it is found that the best isolator performance could exceed 70 dB at a specified incident angle when the nonreciprocal TPPs are excited. Moreover, over the range of frequencies $f = 2.7 - 2.85$ THz, there exist two different incident angles to achieve high isolation in transmission. When the loss in ML is introduced [here in Fig. 8(b) we use a realistic typical value of $\alpha = 0.1$ THz for InSb in the terahertz region], the transmission peaks for both directions are suppressed and broaden, and the non-reciprocity becomes weaker. Nevertheless, the isolation can approach as high as 35 dB, resulting in pronounced non-reciprocity for the proposed structure.

5. Conclusions

In summary, we investigate optical non-reciprocity behaviors associated with asymmetrical TPPs in terahertz MPCs. Nonreciprocal bound TPPs could be supported with a top ML for the MPC, giving rise to the observation of one-way wave propagation at the surface of semi-infinite MPCs. Such non-reciprocity can be attributed to the contribution of direct magnetization effect of surface terminating layer of MPCs. By varying the top layer of MPCs to the dielectric and the other side of the interface by metallic materials, radiative TPPS with non-reciprocity could be seen, originating from the periodicity violation in truncated MPCs. In comparison with the bound TPPs, radiative mode solutions lie inside the light cone for the surrounding materials, and can be well excited directly by incident plane waves, which enables us to see one-way optical tunneling through a finite-size structure. It is expected that those results may provide potential applications on the design of tunable and compact optical isolators. Compared to other metal-dielectric MO structures based on InSb materials that have been proposed for THz isolators [45, 46], the proposed nonreciprocal structure is simple in the geometry design, and compact with thickness less than 100 μm. Meanwhile, our isolator exhibits high non-reciprocity at its operating frequency which can be broadly tuned by changing the incident angles, surface termination as well as external magnetic field.

Funding

Natural Science Foundation of Jiangsu Province (BK20160878, BK20181263); National Natural Science Foundation of China (NSFC) (11774053); The General Research Fund from Hong Kong RGC (15300315).

References

1. R. J. Potton, "Reciprocity in optics," Rep. Prog. Phys. **67**, 717–754 (2004).
2. D. Jalas, A. Petrov, M. Eich, W. Freude, S. Fan, Z. Yu, R. Baets, M. Popović, A. Melloni, J. D. Joannopoulos, M. Vanwolleghem, C. R. Doerr, and H. Renner, "What is and what is not an optical isolator," Nat. Photonics **7**, 579–582 (2013).
3. B. He, L. Yang, X. Jiang, and M. Xiao, "Transmission nonreciprocity in a mutually coupled circulating structure," Phys. Rev. Lett. **120**, 203904 (2018).
4. R. Li and M. Levy, "Bragg grating magnetic photonic crystal waveguides," Appl. Phys. Lett. **86**, 251102 (2005).
5. K. Fang, Z. Yu, V. Liu, and S. Fan, "Ultracompact nonreciprocal optical isolator based on guided resonance in a magneto-optical photonic crystal slab," Opt. Lett. **36**, 4254–4256 (2011).
6. Z. Yu and S. Fan, "Complete optical isolation created by indirect interband photonic transitions," Nat. Photonics **3**, 91–94 (2009).
7. N. A. Estep, D. L. Sounas, J. Soric, and A. Alù, "Magnetic-free non-reciprocity and isolation based on parametrically modulated coupled-resonator loops," Nat. Phys. **10**, 923–927 (2014).
8. H. Lira, Z. Yu, S. Fan, and M. Lipson, "Electrically driven nonreciprocity induced by interband photonic transition on a silicon chip," Phys. Rev. Lett. **109**, 033901 (2012).
9. S. Longhi, "Nonreciprocal transmission in photonic lattices based on unidirectional coherent perfect absorption," Opt. Lett. **40**, 1278–1281 (2015).

Optics EXPRESS

10. F. Ruesink, M. Miri, A. Alù, and E. Verhagen, "Nonreciprocity and magnetic-free isolation based on optomechanical interactions," Nat. Commun. **7**, 13662 (2016).
11. M. Miri, F. Ruesink, E. Verhagen, and A. Alù, "Optical nonreciprocity based on optomechanical coupling," Phys. Rev. Appl. **7**, 064014 (2017).
12. K. Fang, J. Luo, A. Metelmann, M. H. Matheny, F. Marquardt, A. A. Clerk, and O. Painter, "Generalized non-reciprocity in an optomechanical circuit via synthetic magnetism and reservoir engineering," Nat. Phys. **13**, 465–471 (2012).
13. K. Gallo, G. Assanto, K. R. Parameswaran, and M. M. Fejer, "All-optical diode in a periodically poled lithium niobate waveguide," Appl. Phys. Lett. **79**, 314–316 (2001).
14. M. Soljačić, C. Luo, and J. D. Joannopoulos, "Nonlinear photonic crystal microdevices for optical integration," Opt. Lett. **28**, 637–639 (2003).
15. L. Fan, J. Wang, L. T. Varghese, H. Shen, B. Niu, Y. Xuan, A. M. Weiner, and M. Qi, "An all-silicon passive optical diode," Science **335**, 447–450 (2012).
16. Y. Xu and A. E. Miroshnichenko, "Reconfigurable nonreciprocity with a nonlinear Fano diode," Phys. Rev. B **89**, 134306 (2014).
17. F. D. M. Haldane and S. Raghu, "Possible realization of directional optical waveguide in photonic crystals with broken time-reversal symmetry," Phys. Rev. Lett. **100**, 013904 (2008).
18. S. Raghu and F. D. M. Haldane, "Analogs of quantum-Hall-effect edge states in photonic crystals," Phys. Rev. A **78**, 033834 (2008).
19. Z. Wang, Y. Chong, J. D. Joannopoulos, and M. Soljačić, "Observation of unidirectional backscattering-immune topological electromagnetic states," Nature **461**, 772–775 (2009).
20. Y. Poo, R. Wu, Z. Lin, Y. Yang, and C. T. Chan, "Experimental realization of self-guiding unidirectional electromagnetic edge states," Phys. Rev. Lett. **106**, 093903 (2011).
21. Z. Yu, G. Veronis, Z. Wang, and S. Fan, "One-way electromagnetic waveguide formed at the interface between a plasmonic metal under a static magnetic field and a photonic crytal," Phys. Rev. Lett. **100**, 023902 (2008).
22. J. Wang, H. Y. Dong, C. W. Ling, C. T. Chan, and K. H. Fung, "Nonreciprocal μ-near-zero mode in $\mathcal{PT}$-symmetric magnetic domains," Phys. Rev. B **91**, 235410 (2015).
23. M. Kaliteevski, I. Iorsh, S. Brand, R. A. Abram, J. M. Chamberlain, A. V. Kavokin, and I. A. Shelykh, "Tamm plasmon-polaritons: Possible electromagnetic states at the interface of a metal and a dielectric Bragg mirror," Phys. Rev. B **76**, 165415 (2007).
24. I. A. Shelykh, M. Kaliteevski, A. V. Kavokin, S. Brand, R. A. Abram, J. M. Chamberlain, and G. Malpuech, "Interface photonic states at the boundary between a metal and a dielectric Bragg mirror," Phys. Stat. Sol. (a) **204**, 522–525 (2007).
25. M. E. Sasin, R. P. Seisyan, M. A. Kaliteevski, S. Brand, R. A. Abram, J. M. Chamberlain, A. Y. Egorov, A. P. Vasil'ev, V. S. Mikhrin, and A. V. Kavokin, "Tamm plasmon polaritons: slow and spatially compact light," Appl. Phys. Lett. **92**, 251112 (2008).
26. Y. Gong, X. Liu, H. Lu, L. Wang, and G. Wang, "Perfect absorber supported by optical Tamm states in plasmonic waveguide," Opt. Express **19**, 18393–18398 (2011).
27. H. Zhou, G. Yang, K. Wang, H. Long, and P. Lu, "Multiple optical Tamm states at a metal-dielectric mirror interface," Opt. Lett. **35**, 4112–4114 (2010).
28. W. L. Zhang and S. F. Yu, "Bistable switching using an optical Tamm cavity with a Kerr medium," Opt. Commun. **283**, 2622—2626 (2010).
29. K. J. Lee, J. W. Wu, and K. Kim, "Enhanced nonlinear optical effects due to the excitation of optical Tamm plasmon polaritons in one-dimensional photonic crytal structures," Opt. Express **21**, 28817–28823 (2013).
30. A. Kavokin, I. Shelykh, and G. Malpuech, "Optical Tamm states for the fabrication of polariton lasers," Appl. Phys. Lett. **87**, 261105 (2005).
31. C. Symonds, A. Lemaître, P. Senellart, M. H. Jomaa, S. A. Guebrou, E. Homeyer, G. Brucoli, and J. Bellessa, "Lasing in a hybrid GaAs/silver Tamm structure," Appl. Phys. Lett. **100**, 121122 (2012).
32. G. Lheureux, S. Azzini, C. Symonds, P. Senellart, A. Lemaître, C. Sauvan, J. Hugonin, J. Greffet, and J. Bellessa, "Polarization-controlled confined Tamm plasmon laser," ACS Photonics **2**, 842–848 (2015).
33. O. Gazzano, S. M. de Vasconcellos, K. Gauthron, C. Symonds, P. Voisin, J. Bellessa, A. Lemaître, and P. Senellart, "Single photon source using confined Tamm plasmon modes," Appl. Phys. Lett. **100**, 232111 (2012).
34. R. Badugu, E. Descrovi, J. R. Lakowicz, "Radiative decay engineering 7: Tamm state-coupled emission using a hybrid plasmonic-photonic structure," Anal. Biochem. **445**, 1–13 (2014).
35. Y. Chen, D. Zhang, D. Qiu, L. Zhu, S. Yu, P. Yao, P. Wang, H. Ming, R. Badugu, and J. R. Lakowicz, "Back focal plane imaging of Tamm plasmons and their coupled emission," Laser Photonics Rev. **8**, 933–940 (2014).
36. Y. Chen, D. Zhang, L. Zhu, R. Wang, P. Wang, H. Ming, R. Badugu, and J. R. Lakowicz, "Tamm plasmon- and surface plasmon-coupled emission from hybrid plasmonic-photonic structures," Optica **1**, 407–413 (2014).
37. M. Tonouchi, "Cutting-edge terahertz technology," Nat. Photonics **1**, 97–105 (2007).
38. S. Lin, K. Bhattarai, J. Zhou, and D. Talbayev, "Thin InSb layers with metallic gratings: a novel platform for spectrally-selective THz plasmonic sensing," Opt. Express **24**, 19448–19457 (2016).
39. M. Mandehgar, Y. Yang, and D. Grischkowsky, "Atmosphere characterization for simulation of the two optimal wireless terahertz digital communication links," Opt. Lett. **38**, 3437–3440 (2013).

Optics EXPRESS

40. J. G. Rivas, C. Janke, P. H. Bolivar, and H. Kurz, "Transmission of THz radiation through InSb gratings of subwavelength apertures," Opt. Express **13**, 847–859 (2005).
41. B. Hu, Q. J. Wang, and Y. Zhang, "Broadly tunable one-way terahertz plasmonic waveguide based on nonreciprocal surface magneto plasmons," Opt. Lett. **37**, 1895–1897 (2012).
42. H. Y. Dong, J. Wang, and T. J. Cui, "One-way Tamm plasmon polaritons at the interface between magnetophotonic crystals and conducting metal oxides," Phys. Rev. B **87**, 045406 (2013).
43. A. B. Khanikaev, A. V. Baryshev, M. Inoue, and Y. S. Kivshar, "One-way electromagnetic Tamm states in magnetophotonic structures," Appl. Phys. Lett. **95**, 011101 (2009).
44. B. H. Cheng, H. W. Chen, K. J. Chang, Y. Lan, and D. P. Tsai, "Magnetically controlled planar hyperbolic metamaterials for subwavelength resolutions," Sci. Reports **5**, 18172 (2015).
45. F. Fan, S. Chen, X. Wang, and S. Chang, "Tunable nonreciprocal terahertz transmission and enhancement base on metal/magneto-optic plasmonic lens," Opt. Express **21**, 8614–8621 (2013).
46. S. Chen, F. Fan, X. Wang, P. Wu, H. Zhang, and S. Chang, "Terahertz isolator based on nonreciprocal magneto-metasurface," Opt. Express **23**, 1015–1024 (2015).